Transit Method Analysis for Exoplanet Detection Validation Observations for TESS Object of Interest 3553.01

Jayarsh Singh, Peter Plavchan, and Kevin Collins

Department of Physics and Astronomy, 4430 University Drive MS 3F3, George Mason University, Fairfax, VA 22030, USA

ABSTRACT

The goal of this observational research was to further develop a conclusion for the confirmation of TIC 239628993 (TOI 3553.01) as an exoplanet, originally detected by the Transiting Exoplanet Survey Satellite (TESS). We used the transit method to measure the light emitted from a system's host star and plotted data values throughout the exoplanet's transit. To increase the effectiveness of the transit method, we used image calibration, stack editing, image stabilization/alignment, interactive macro settings, multi-aperture photometry, and differential photometry, all supplied via the software AstroImageJ. Using the features of AstroImageJ, we compared the emitted light of the target star to those of numerous surrounding stars, and generated light curves consisting of normalized and best-fit data. Based on the best-fit modeled light curve, TIC 239628993 (TOI 3553.01) was classified as an exoplanet However, the light curve showed that the host star's brightness consistently decreased towards the end of the data set, not showing the returning increase of brightness. The decrease in emitted light was deemed sufficient to further support the classification of TIC 239628993 as an exoplanet, but based on these tentative results, the transit of the exoplanet as it passed in front of its host star was rendered an incomplete (partial) transit.

1. INTRODUCTION

Celestial bodies outside of our solar system have inspired astronomers to search beyond our current understanding of the universe. The study of exoplanets remains a core field of research due to the goal of studying the atmosphere of various planets, learning more about the origins of the universe, and finding extraterrestrial life/planets that are able to host living organisms(1). Exoplanets are planets that orbit a host star that is outside of our solar system, and they are able to be detected due to the temporarily decreasing brightness of a star as the planet passes in front of it. These exoplanet transits are measurable, and are therefore able to be detected using predicted ingress (when the planet will start passing in front of its host star) and egress (when the planet will finish passing in front of its host star) times (2).

Advanced technology has allowed researchers to investigate exoplanets more thoroughly. The Transiting Exoplanet Survey Satellite (TESS) is a major example of the rapid development of exoplanet research. The TESS mission was launched by the National Aeronautics and Space Administration (NASA) in 2018, surveying the sky with the goal of finding thousands of exoplanets around nearby dwarf stars. TESS has identified 6,788 potential exoplanet candidates, and confirmed 383 candidates as exoplanets (3). TESS primarily uses the transit method to identify potential exoplanet candidates by measuring consistent, periodic decreases in the amount of light emitted from a host star. TESS uses four specific cameras to collect data from nearby stars (4). This data is used to find any possible transits of an exoplanet candidate in front of its host star, blocking a portion of light that gets captured via TESS's cameras. Once confirmed, the data is used to determine the planet's diameter and orbital radius, which can be used for calculating the ingress and egress times. The "habitable zone" is a specific range of the planet's orbit around the host star where liquid water exists on the planet, thus making the exoplanet a possible area for humans to inhabit (4), one of the main areas of discovery that TESS was launched for. The TESS validation process begins with data being transferred to the Payload Operations Center (POC) in Massachusetts. The

Deep Space Network (DSN) downloads the data before being sent to the POC, and the final data is calibrated and analyzed by the Science Processing Operations Center (SPOC) (5). The final data is analyzed in greater depth by follow-up observations in order to confirm whether an exoplanet candidate clears the validation process to be classified as an exoplanet (6).

In this paper, we present follow-up observations of TOI 3553.01. This TESS candidate orbits its stellar host, TOI 3553, and has a radius of approximately 11.823 R⊕. TOI 3553.01 has an orbital period of approximately 1.94 days. The transit duration of the exoplanet is approximately 1.77 hours, and the predicted transit depth is approximately 0.4846 %. The host star TOI 3553 has a stellar radius of 1.46 R⊙, and has a stellar effective temperature of 6497.2 K (7). The goal of this paper is to use follow-up observations and analysis using TESS mission data on TOI 3553.01 to determine if the transit of the exoplanet candidate occurred.

In section 2, we present our procedures and observations taken from the George Mason University 0.8m telescope. In section 3, we present the analysis of the tools we used through AstroImageJ (AIJ) in order to generate the light curve, and the data taken from multi-aperture photometry. In section 4, we present the results taken from the analysis. In section 5, we present the discussion proving an explanation of the data collected and analyzed, as well as concluding whether or not a transit of TOI 3553.01 passing in front of its host star occured. In section 6, we discuss conclusions from research and observations, along with plans for future work.

2. OBSERVATIONS

In section 2.1, we present the data reduction processes for the initial raw images collected from the George Mason University 0.8m telescope. In section 2.2, we present the processes for plate-solving, performing aperture photometry, performing multi-aperture photometry, and using these processes to generate light curves.

2.1

We collected raw science images using the George Mason University 0.8m telescope. There were 303 total exposures collected, with a 60 second exposure time for each science, all observed using the R filter. The start time was 20:40 on August 30, 2022, and the end time was 05:40 on August 31, 2022, resulting in a 5-hour science capture duration (7). The Right Ascension (RA) value was 21h, 42m, 24.91s. The Declination (Dec) value was +29d, 52m, 09.75s.

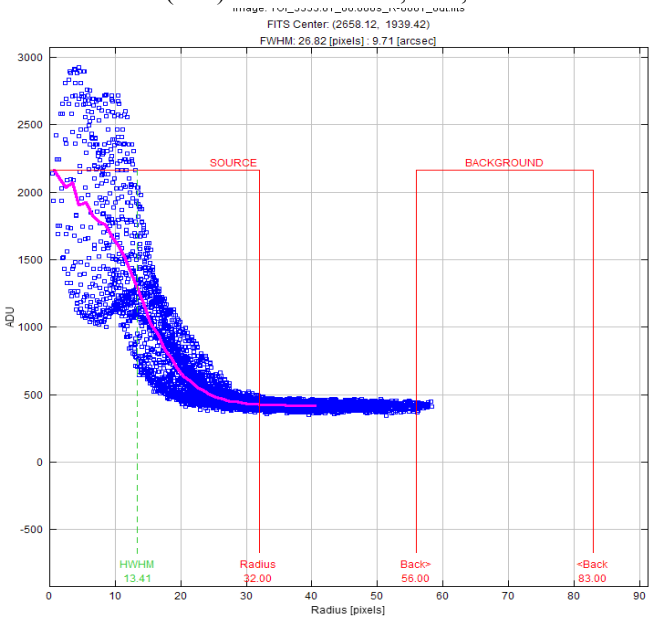

Figure 1. Seeing profile for the plate-solved image stack.

2.2

Following the collection of raw science data, the images were plate-solved using the external server "Astrometry.net", meaning each raw image was compared to a star field from a database of various star positions. Before using the plate-solved images to perform aperture photometry, we removed 17 "bad" images that were corrupted due to satellite streaks and excessive cloud cover. Using AstroImageJ, we stacked the plate-solved images and opened the seeing profile **(Figure 1),** which gave us the values to use for the aperture size, inner radius of background annulus, and outer radius of background annulus. The "Radius" in figure 1 was set as the value for the aperture size, which was 32. The "Back>" value was set as the inner radius of background annulus, which was 56. The "Back<" value was set as the outer radius of background annulus, which was 83. We used these values when apertures were placed for reference stars to generate onto the image stack screen, allowing us to gather data on reference stars nearby the host star TOI 3553, which let us to compare and analyze the transit data of exoplanet candidate TOI 3553.01 more thoroughly. After all apertures were placed, the measurements began to run, plotting all the data from the plate-solved sciences as well as reference star data for comparison, and using this data to generate a light curve.

3. ANALYSIS

In section 3.1, we present the different tools and settings used in AstroImageJ to analyze the light curve generated by the data given from multi-aperture photometry. In section 3.2, we present our analysis of the ground-based light curve generated through AstroImageJ. In section 3.3, we talk about the process of correctly plotting the data in order to effectively compare the light curves of our target star and our reference stars. In section 3.4, we discuss the methods for detrending the data to remove any externalities that may have occurred during the data collection process.

3.1

When analyzing the data shown on the light curve, we edited the formatting of the curve using AstroImageJ settings. The "data set" window helped shift the light curve by selecting items to detrend which means some systematic trends were removed. These can include brightness in the sky, atmosphere problems, telescope shifts, or environmental issues (9). The axes and scaling of the entire graph was also altered - the maximum and minimum height of the graph would either decrease or increase the y-values associated with the graph, thus stretching or shrinking each light curve.

3.2

To analyze the emitted light based on the transit light curve, we fitted the light curves based on detrending different systematic trends and observed dips in data along the data set. We compared the fitted curve of the host star TOI 3553 before, during, and after the exoplanet candidate passed in front of it. We compared this fitted curve to nearby reference stars light curves, all of which have not been detrended. We used the predicted ingress and egress times to review if the light curve of the target star dipped in relative flux.

3.3

Following the collection of the light curve data, we scaled the x and y axes in order to fit every point of data that was generated. The scales of the reference stars were contracted in order to make space for the complete light curve of the target star, as well as a second light curve of the target star which was not detrended.

3.4

When detrending the data, there are many different trends that affect the way the data is portrayed on the light curves. The trend "Width_T1" calculates the mean of the x-direction and y-direction FWHM of our target star. FWHM (Full-Width half maximum) describes the amount that a point of light spreads out, and it is used to describe seeing

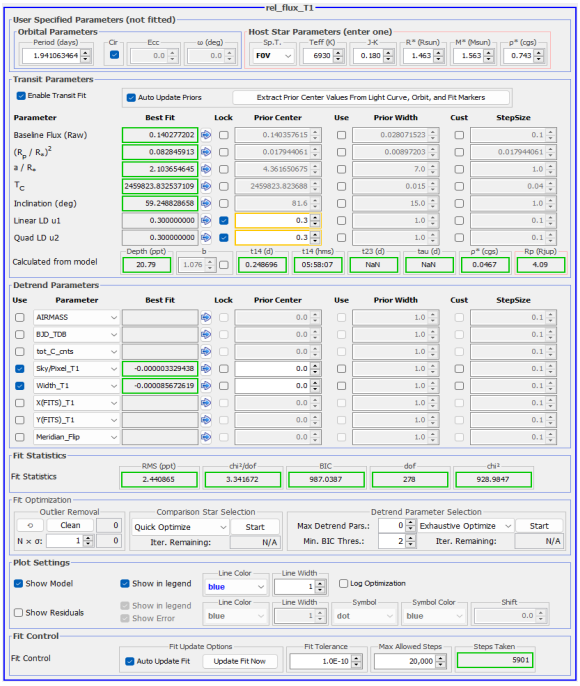

Figure 2: Different data given by the main light curve, based on different options to detrend.

conditions/level of atmospheric turbulence in the night sky. The "Sky/Pixel_T1" describes variation in the background sky, generally due to system settings of the telescope capturing and collecting data. The "Airmass" and "Tot_C_cnts" trends show the transparency level during the observation (10). The light curve of our host star only detrended the "Sky/Pixel" and "Width" trends, as it shifted the curve to exemplify a clear transit **(Figure 2)**.

4. RESULTS

In section 4.1, we discuss the plot of all measurements that were collected and plotted onto the final graph. In section 4.2, we discuss a separate graph consisting of two light curves, each a variation of our target star. In section 4.3, we present a graph containing 3 light curves, all of our target stars, each representing a different aperture size (aperture radius, inner sky, and outer sky). These are all measures of the area of the sky surrounding our target star image capturing/calibration during observing.

4.1

In the final graph of edited light curves, we included the light curve of our host star (detrended), light curve of our host star (not detrended), reference

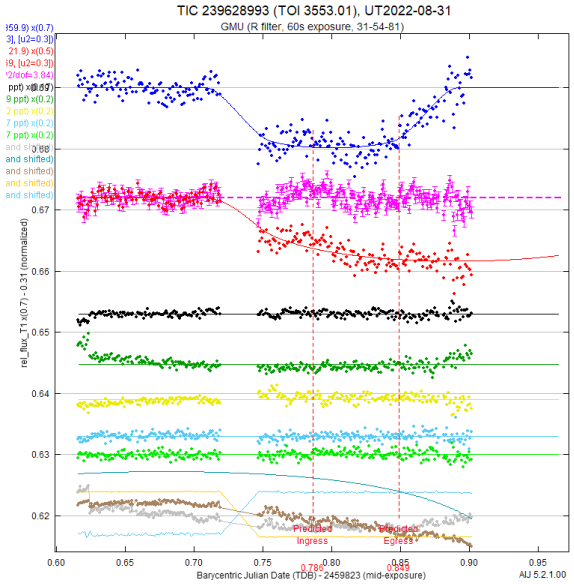

Figure 3: Final graph of all measurement data collected: Detrended/non-detrended light curves of the host star, light curves for each reference star, and light curves for each individual trend.

stars, light curve of the "Width_T1" trend, light curve of the "Sky/Pixel_T1" trend, light curve of the "Airmass" trend, light curve of the "Tot_C_cnts" trend, and light curve of the "Y(Fits)_T1" trend. The scales of the light curves of the various trends are all fitted the smallest in order to emphasize the transit qualities of the main light curve for our host star, as well as compare it to the other reference stars, which were only slightly scaled down **(Figure 3).**

4.2

To conduct a better analysis of the data collected, we produced a graph that compared two light curves of the target star: one that was detrended with 2 trends ("Width_T1" and "Sky/Pixel_T1), and one that was not detrended **(Figure 4)**. This comparison helped differentiate the effects that different systematic and/or natural trends had on the data that was originally generated into a plot.

4.3

Prior to adjusting any settings pertaining to any light curve, a general summary of the light curve appeared, in order to verify that the AIJ light curve generator was successful **(Figure 5).** The blue curve represents the images taken in the field of view of the target star´s radius (32). The green curve represents the images taken in the field of view of the radius of a small section of the sky surrounding the star, which is called the ¨inner sky¨ (56). The red curve represents the images taken in the field of view of the radius of a

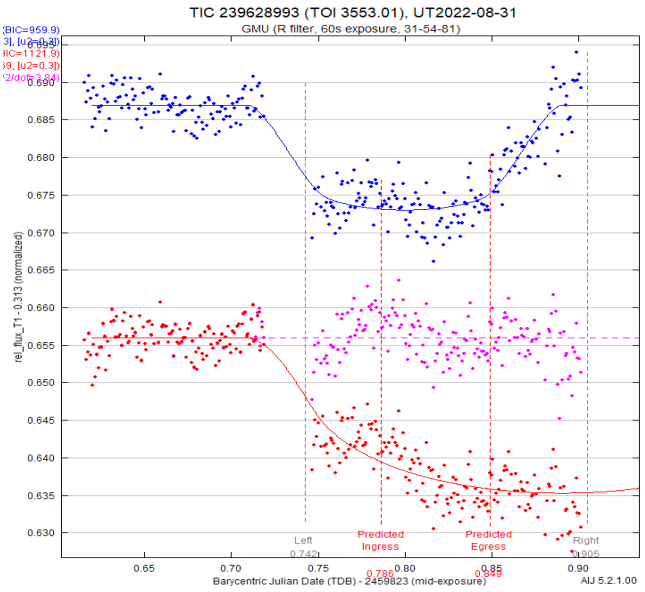

Figure 4: A graph comparing two light curves from the main star. The blue curve is detrended with "Width_T1" and "Sky/Pixel_T1", while the red curve is not detrended.

a large section of the sky surrounding the target star, known as the ¨outer sky¨ (83).

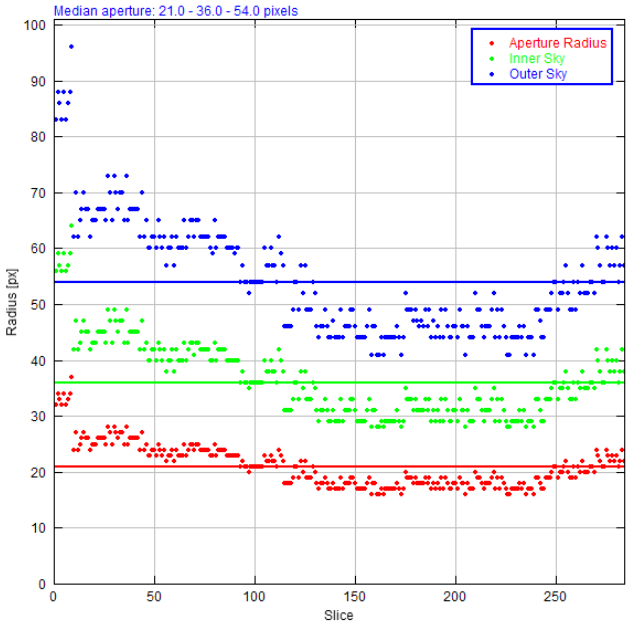

Figure 5: A graph of 3 general summary light curves of the same target star, prior to any settings adjustment. The curves represent the data collected with the area size of the target star's radius, the ¨inner sky¨portion, and the ¨outer sky¨portion.

5. DISCUSSION

In section 5.1, we discuss the classification of the transit that occurred. In section 5.2, we discuss the details of ingress and egress times predicted by an AIJ model.

5.1

The variation in flux data given from the AIJ-generated light curves shows that there was a transit from TOI 3553.01 passing in front of its host star. The relative flux for each reference star stays within 0.05 ppt (parts per trillion) of the line of best fit, while the relative flux emitted from our target star during the transit of TOI 3553.01 decreased by approximately 0.1 ppt. However, there is a gap in the light curve from our target star from 0.72 BJD through 0.74 BJD **(Figure 3).** The images (known as bad images) containing data for this time range were removed before plate-solving and generating the light curve due to atmospheric turbulence, satellite streaking, or faults from the observatory telescope. The removal of the images resulted in there being no data on the light curve for a small portion of the beginning of the transit, but doesn't impact the overall compensation of the light curve. However, when looking at the light curve that is not detrended **(Figure 4)**, the light curve ends approximately 60% of the way through the transit, meaning that image data was not collected nor calibrated past this point. This led to the conclusion that TOI 3553.01 underwent a partial transit (incomplete).

5.2

As the graph of the light curves was analyzed **(Figure 4)**, we discovered that the ingress and egress times (that were predicted through the AIJ data calibrator and generator) were misaligned with the true ingress and egress time shown by the light curve. The predicted ingress and egress times generated through AIJ were 0.786 BJD and 0.849 BJD, respectively. Uncertainties regarding the predicted ingress and egress times occur more frequently at high observatory altitudes due to possible atmospheric refraction (11). The true ingress and egress times based on the data portrayed on the light curve **(Figure 4)** are approximately 0.703 BJD and 0.902 BJD, meaning that the predicted ingress time had an absolute error of approximately 0.38%, and the predicted egress time had an absolute error of approximately 5.89%. These calculations were made based on the following formula:

$$\delta = \left[\frac{V_a - V_e}{V_e}\right] \times 100\%$$

δ is percent error, V_a is the observed value, and V_e is the expected value (12).

6. FUTURE WORK

In section 6.1, we discuss future plans for statistical validation (through the analysis of NEB data) for confirming TOI 3553.01 as an exoplanet.

6.1

Analyzing light curves generated through image calibration data is deemed adequate, but on its own will not serve as enough evidence to confirm a transiting exoplanet. Testing for false-positives will further remove any doubts concerning the validity of the transit. While we were unable to access an NEB (Nearby-Eclipsing Binary) file through AIJ during our research, in the future we plan on creating an NEB file containing data from neighboring stars, with the goal of eliminating the possibility of the exoplanet transit being corrupted by data from nearby stars.

7. ACKNOWLEDGEMENTS

We would like to thank Dr. Peter Plavchan (Department of Physics and Astronomy, George Mason University) for guiding us through this research and expanding our shared passion for astronomy and the wonders of the universe. We would also like to thank the George Mason University staff for allowing us to use their on-campus observatory telescope and other resources.

8. REFERENCES

1. ESA, "What are Exoplanets?", European Space Agency, 2023, https://www.esa.int/Science_Exploration/Space_Science/Exoplanets/What_are_exoplanets#:~:text=Studying%20the%20diverse%20range%20of,provides%20essential%20clues%20towards%20understanding

2. Roger Dymock, “Exoplanet Transit Imaging and analysis Process”, British Astronomical Association, 2018, https://britastro.org/section_information_/exoplanets-section-overview/exoplanet-transit-imaging-and-analysis-process

3. Pat Brennan, “Transiting Exoplanet Surveying Satellite (TESS)”, NASA, 2021, https://exoplanets.nasa.gov/tess/#:~:text=The%20Transiting%20Exoplanet%20Survey%20Satellite,drops%20caused%20by%20planet%20transits

4. NASA, “Transiting Exoplanet Surveying Satellite (TESS)”, Harvard and Smithsonian, https://exoplanets.nasa.gov/tess/#:~:text=The%20Transiting%20Exoplanet%20Survey%20Satellite,drops%20caused%20by%20planet%20transits

5. Thomas Barclay, “TESS Data Processing Pipeline”, NASA, 2023, https://exoplanets.nasa.gov/tess/#:~:text=The%20Transiting%20Exoplanet%20Survey%20Satellite,drops%20caused%20by%20planet%20transits

6. Joshua Schlieder, “Follow-Up and Validation of K2 and TESS Planetary Systems With Keck NIRC2 Adaptive Optics Imaging”, Frontiers, 2021, https://www.frontiersin.org/articles/10.3389/fspas.2021.628396/full

7. Ipac, “NASA Exoplanet Archive”, NASA, 2023, https://exoplanetarchive.ipac.caltech.edu/overview/TOI-3553.01#planet_TOI-3553-01_collapsible

8. Danny Goode, “Plate Solving”, Stargazers Lounge, 2019, https://exoplanetarchive.ipac.caltech.edu/overview/TOI-3553.01#planet_TOI-3553-01_collapsible

9. Karen Collins, “AstroImageJ User Guide”, NASA Kentucky, 2016, https://exoplanetarchive.ipac.caltech.edu/overview/TOI-3553.01#planet_TOI-3553-01_collapsible

10. Dennis Conti, “TFOP_SG1_Guidelines”, AstroImageJ, 2020, https://exoplanetarchive.ipac.caltech.edu/overview/TOI-3553.01#planet_TOI-3553-01_collapsible

11. CalTech, “Transit Tips and Troubleshooting”, California Institute of Technology, 2020, https://exoplanetarchive.ipac.caltech.edu/overview/TOI-3553.01#planet_TOI-3553-01_collapsible

12. “Percent Error Calculator”, Calculator Soup, 2023, https://www.calculatorsoup.com/calculators/algebra/percent-error-calculator.php

13. Ravi Kopparapu, “Exoplanet Classification and Yield Estimates for Direct Imaging Missions”, The Astrophysics Journal, 2018, https://iopscience.iop.org/article/10.3847/1538-4357/aab205#:~:text=Broadly%2C%20the%20planets%20are%20divided,on%20the%20incident%20stellar%20flux

14. Sarah Tang, “Ground-based Follow-up Observations of TESS Exoplanet Candidates”, Journal of Emerging Investigators, 2020, https://emerginginvestigators.org/articles/ground-based-follow-up-observations-of-tess-exoplanet-candidates/pdf